Volume 9, Issue 3, 2019, 3942 - 3948 **ISSN 2069-5837**

Biointerface Research in Applied Chemistry

www.BiointerfaceResearch.com

https://doi.org/10.33263/BRIAC93.942948

Original Research Article **Open Access Journal**

Received: 26.04.2019 / Revised: 25.05.2019 / Accepted: 06.06.2019 / Published on-line: 15.06.2019

Comparative spectroscopic analysis of nordihydroguaiaretic acid and related natural products to inhibition of calcium oxalate calculi

Felicia S. Manciu [1, 2, 3, *], John D. Ciubuc [1, 2], Katia Ochoa [1], Preethi Dacha [1], Mahendra Subedi [1], Jose Guerrero [1], Michael Eastman [4], Deidra R. Hodges [5], Kevin E. Bennet [6, 7]

[1]Department of Physics, University of Texas at El Paso, El Paso, TX 79968, USA
[2] Department of Biomedical Engineering, University of Texas at El Paso, El Paso, TX 79968, USA
[3] Border Biomedical Research Center, University of Texas at El Paso, El Paso, TX 79968, USA
[4] Department of Chemistry, University of Texas at El Paso, El Paso, TX 79968, USA
[5] Department of Electrical and Computer Engineering, University of Texas at El Paso, El Paso, TX 79968, USA
[6] Division of Engineering, Mayo Clinic, Rochester, MN 55905, USA
[7]Department of Neurologic Surgery, Mayo Clinic, Rochester, MN 55905, USA

*corresponding author e-mail address: ***fsmanciu@utep.edu***

ABSTRACT

The prevalence of urolithiasis is still increasing worldwide. The goal of this study is to achieve a better understanding, from a comparative spectroscopic perspective, of the differences provided by chemical and natural products to the inhibitory processes of calculi formation. The research presented here places primary emphasis on the assessment of nordihydroguaiaretic acid (NDGA), the main chemical extract of the plant *Larrea Tridentata*, as a preventative to calcium oxalate crystal formation. It is also a logical continuation of our previous efforts using a traditional medicine approach to study such prevention. Complementary Raman and Fourier transformed infrared (FTIR) absorption analysis were used to provide a complete overview of morphological changes of calcium oxalate crystals, which were grown without and with the addition of NDGA at different concentrations. A gel diffusion technique was employed for sample preparation. Our results from both Raman and FTIR spectroscopies demonstrate that no structural transformation from a monohydrate to dehydrate occurs upon crystallization with NDGA, as we previously reported for the use of the natural plant infusion. Calculi synthesized with NDGA shows a distorted monohydrate morphology. Different effects inhibitory to calcium oxalate calculi formation are observed and analyzed here using chemical and natural extracts. If magnesium is the key to this difference, this study confirms its importance, not only in hundreds of metabolic pathways, but also in nephrological ones.

Keywords: *urinary calculi; Raman spectroscopy; FTIR; structure-property relationship; nordihydroguaiaretic acid; natural products.*

1. INTRODUCTION

Urolithiasis, more commonly known as kidney stone disease, is a globally growing urological disorder, affecting approximately 3-15% of the world's population with nearly one in every 11 individuals developing the disease [1,2]. Furthermore, more than half of individuals diagnosed with urinary calculi will see reoccurrence of the disease within 5-10 years [2]. Urinary calculi consist of hard masses, with surfaces varying in smoothness and irregularities, and are located primarily within the kidney [3]. Although the exact mechanism behind urinary calculi formation is not completely understood, several etiologic factors have been successfully identified. Such factors include genetic influence, super-saturated urine, epithelium alterations in the renal papilla, and food habits combined with lifestyle [2,3]. The disease is very likely to cause significant pain for the individual, leading to a substantial negative impact on society, work environments, and healthcare systems. Management of the disease in the employed population within the United States was estimated to cost $5 billion dollars in the year 2000 [4,5]. Urolithiasis has been associated with high-risk diseases, including chronic kidney disease [6], cardiovascular disease [7], hypertension [8], obesity [8,9], diabetes [10], and end-stage renal failure [11,12]. Whilst no causal connection has been discovered between urolithiasis and the aforementioned diseases, treatment of one of the disorders may prevent the occurrence of some of the others [2,13,14].

The composition of urinary calculi can be divided into in two categories: the organic matrix and the mineral component. The organic matrix consists primarily of amino acids, carbohydrates, and lipids, while the mineral component assumes various identities depending on the classification of the calculi [3]. Over 80% of urinary calculi contain calcium compounds, with calcium oxalate and calcium phosphate being the primary contributors [3]. The chemical components of the remaining 20% are of either uric acid or struvite origin, with a small percentage falling into several different classifications, such as those having cystine and drug related origins [3]. When the urine's pH balance becomes too acidic or too basic, this causes accumulation of minerals that form kidney stones. Researchers suspect that high protein diets might also cause stone formation since, during digestion of proteins, acids are created. The body balances the acidity with the available alkaline base: calcium (having its reservoir in bones). This could result in deposition of calcium in the kidneys and its accumulation could form kidney stones [15-18]. Generous fluid (water) intake could prevent high concentrations of stone precursors in the urine, and thus could reduce the risk of kidney stone formation. In addition, water is the active fluid for passing small stones through the ureter. Thus, determining the exact composition of urinary calculi can lead to

the identification of causation, which in some cases may be the only means of discovering the origin of the disorder [19] .

Despite significant progress in modern medicine, especially in developed countries, the prevalence and recurrence rate of urolithiasis is still increasing worldwide, with 50% more cases over the past 10 years; its occurrence in 2017 was more than twice that of 1994 [1,2,5]. Furthermore, the high cost of clinically available methods of urolithiasis diagnosis and treatment, as well as some of the side effects of currently administered drugs, have induced greater public utilization of traditional herbal medicine. In this context it also worth mentioning that poorly informed use of traditional medicine, such as consumption of various natural medications, used mainly as dietary supplements, can also have detrimental side-effects [20-22]. Nevertheless, recent scientific studies have confirmed positive effects from using traditional herbal medicine for inhibiting these urinary disorders [17,23-26].

Many different methods have been applied to urinary calculi characterization, with spectroscopic techniques such as Fourier transform infrared (FTIR) spectroscopy and Raman spectroscopy still leading such analysis [24-29]. Despite the advantages brought by these methods of investigation of urinary calculi formation, difficulties with oxalate hydrate discrimination still exist [27]. The two primary hydrates in calcium oxalates are calcium oxalate monohydrate (COM), whewellite, and calcium oxalate dihydrate (COD), known as weddellite [3,27]. Discrimination between the two calcium oxalate hydrates is important, as they may indicate different pathogenetic outcomes. Specifically, if only a single hydrate type is present, this is a symptom of hyperoxaluria, whereas renal lithiasis may occur in the presence of multiple hydrate types [30-32]. The two hydrates are easily distinguishable in spectroscopic data, from variances in characteristic signatures (singlets for COD compared to doublets for COM) and peak intensities in key frequency regions [28]. Weddellite contains equivalent planar units of oxalate, whereas whewellite contains two types of oxalate unit: one planar and the other slightly twisted, with shorter C–C distances [28].

The research presented here places particular emphasis on understanding, from a comparative spectroscopic perspective (*i.e.* using Raman and infrared absorption spectroscopies), the potential inhibitory effect of nordihydroguaiaretic acid (NDGA) on the formation of calcium oxalate crystals. NDGA, also known as masoprocol, is a chemical extract of the *Larrea Tridentata* bush, a plant that belongs to the *Zygophyllacea* family and is traditionally employed in the El Paso region as a natural treatment for kidney stones and bladder diseases [21,24,33-35]. While NDGA is present in the whole plant, its primary distribution is on the surfaces of the leaves, the flowers, and the green stems [21]. Our previously reported spectroscopic results on such inhibitory processes by *Larrea Tridentata* herbal infusion confirmed significant decreases in crystal sizes [24]. Also, morphological differences, from a monohydrate versus a dehydrate, for pure calcium oxalate versus crystals grown with the inhibitor, respectively, were observed. Thus, the research reported here is a logical continuation of our previous efforts to fathom this complex process, which is far from being completely understood. Particularly, we seek to confirm whether NDGA, a proven antioxidant, is mainly responsible for this inhibitory process. This work could also add important value to the future pharmaceutical applicability of NDGA to kidney stone treatments and drug delivery.

2. MATERIALS AND METHODS

2.1. Materials and sample preparation.

Although, a multitude of methods for growing calcium oxalate crystals in the laboratory are available in the literature, for the sake of comparison with our previously reported results [24], the diffusion gel growth technique was used again for the current means of sample preparation. The synthesis of the samples is similar to the one used for growing calculi with and without the *Lareea Tridentata* herbal extract [24], the modification being the employment of different concentrations of NDGA, in this case. A description of the sample preparation is as follows: calcium chloride ($CaCl_2$) and potassium oxalate ($K_2C_2O_4\,H_2O$) purchased from Sigma-Aldrich (Sigma-Aldrich Co.) were used to prepare two different 0.4M stock solutions by mixing 8.879g of $CaCl_2$ and 14.739g of $K_2C_2O_4{\cdot}H_2O$, each in separate beakers, with 200ml of milli-Q water (of 18.2 MΩ·cm resistivity at room temperature) under vigorous stirring in order to assure solution homogeneity. To each stock solution, 22.848g of Knox gelatin (Kraft Foods Global Inc, Tarrytown, NY) was added under vigorous stirring and moderate heat to form a melted gelatin solution. The pH of these gel solutions was adjusted to 5.5 by titration with small volumes of concentrated HCl (10M).

The $CaCl_2$ gel was then equally divided into eight glass tubes, each containing 25ml and left to cool until the gelatin congealed. Next, 0.3ml aqueous NDGA solutions, at concentrations of 25µM, 50µM, 75µM, 100µM, 250µM, 500µM, and 1mM were gently poured into a different one of these glass tubes. To the eight glass tube, the control, was added 0.3ml of milli-Q water. Then, 25ml of the 0.4M potassium oxalate gel solution was poured on top, into each tube. The glass tubes were covered tightly with paraffin film to allow the formation of crystals through a diffusion process at the gel-liquid interface. After a few weeks the resulting crystals were harvested and analyzed. Prior to their characterization, the crystals were sonicated for 10 minutes in milliQ water to remove the excess of gelatin and impurities.

2.2. Experimental set-up and data acquisition.

The Raman and Fourier transformed infrared (FTIR) spectroscopic measurements were performed at room temperature, under ambient conditions and in vacuum, respectively. For the acquisition of Raman spectra, an *alpha 300RAS WITec* system (WITec GmbH, Ulm, Germany) equipped with a frequency-doubled neodymium-doped yttrium–aluminum–garnet (Nd:YAG) laser (λ = 532nm) and a 20X air objective lens (Olympus, Japan)

with a numerical aperture (NA) of 0.4 was used. The laser power was kept at an output of a few mW. Local accumulations of 20 Raman spectra, with each spectrum acquired in 500 milliseconds, for total acquisition times of 10 seconds and spectral resolutions of 4 cm^{-1}, were performed. For each sample, to compensate for the expected inhomogeneity and for better comprehension of potential morphological changes with NDGA usage, Raman data were collected in different spots and on different crystals; the averages of these Raman spectra are presented and further analyzed below. Appropriate background subtraction was applied to all spectra. Also, the Raman spectra of $CaC_2O_4{\cdot}(H_2O)_x$ crystals were normalized to the strongest intensity of the characteristic doublet peak at 1465 cm^{-1}. A Bruker IFS 66v FTIR spectrometer was employed for IR transmission experiments with a resolution of 4 cm^{-1} and in a frequency range of 400 to 4000 cm^{-1}. Each IR spectrum resulted from an accumulation of 256 scans. The KBr pellet technique was used for such measurements.

3. RESULTS AND DISCUSSION

Controlled nucleation is observed in Fig. 1a and b, where representative images of the formation of crystals are presented. Besides the presence of a white crystalline layer in Fig. 1a, which demonstrates that the growth process occurs mainly at the interface between the two media, additional formation of small crystallites (some marked by black arrows in Fig. 1b) is also observed.

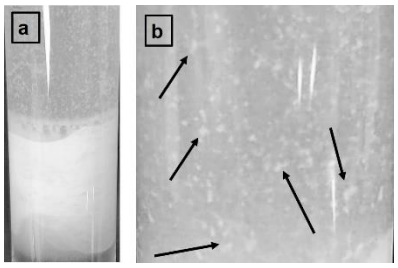

Figure 1. (a) and **(b)** Representative images of controlled nucleation and formation of calcium oxalate crystals through a gel diffusion method. The arrows mark the formation of crystallites in the gel medium.

Evidence of the inhibitory effect of NDGA on the average crystal size is shown in Fig 2a-c. A reduction in average size from 1.2mm for pure $CaC_2O_4{\cdot}(H_2O)_x$ crystals to a maximum of 0.5mm for crystals grown with 1mM NDGA is observed. However, these images reveal formation of agglomerates of crystallites, of spherical shapes for pure $CaC_2O_4{\cdot}(H_2O)_x$ and with an overall "cauliflower-like" aspect for the irregularly aggregates grown with NDGA. Thus, this assessment of crystal sizes is just a coarse approximation.

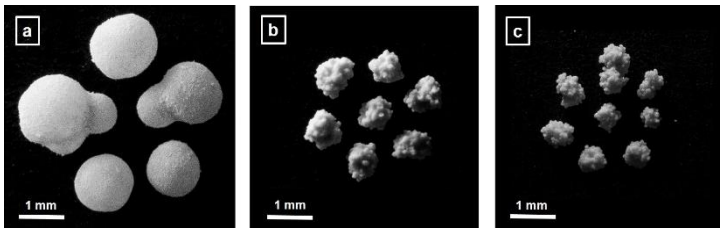

Figure 2. (a) Standard crystals grown without the NDGA inhibitor. **(b)** and **(c)** Evidence of the inhibitor's effect on crystals' sizes and their tendency toward agglomeration for 500μM and 1mM concentrations of NDGA, respectively.

Selective Raman results for calcium oxalate crystals grown without or with different amounts of NDGA (as labeled), as well as the Raman spectrum of NDGA itself, which is shown for comparison, are presented in Fig. 3 a and b, respectively. A break between 2100 and 2500 cm^{-1} is applied to all spectra to allow inclusion of all regions of interest in the same figure. Also, for easier visualization, vertical and horizontal translations were applied to the Raman spectra of calcium oxalate crystals. At a glance, the addition of NDGA does not make visible changes in the Raman vibrational lines of the crystals grown with this compound; only the characteristic vibrations of pure $CaC_2O_4{\cdot}(H_2O)_x$ are seen in all these spectra. Also, no NDGA presence is depicted in the calcium oxalate Raman spectra, not even for the strongest vibrational lines of this compound around 800 cm^{-1}. A potential explanation for the absence of NDGA's Raman signatures could be the Raman sensitivity limit in detecting low concentrations of analytes.

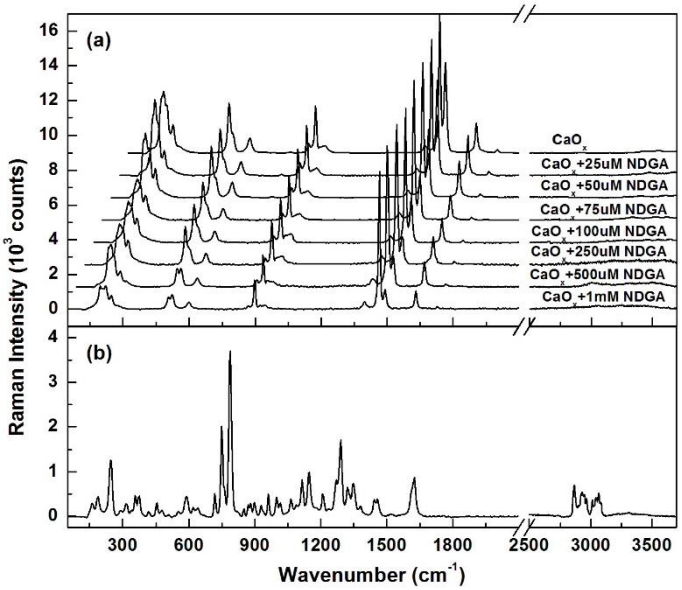

Figure 3. (a) Raman spectra of crystals without and with different amounts of NDGA inhibitor, as labeled, and **(b)** the Raman spectrum of the NDGA alone.

Even for the addition of 0.3 ml of 1mM, the highest concentration of NDGA, to an overall 50ml of gel solution of $CaCl_2$ and $K_2C_2O_4{\cdot}H_2O$, the resulting NDGA concentration of about 6μM is very low for standard Raman detection. The existence of a strong peak doublet in the frequency range of 1450 – 1500 cm^{-1} in these spectra, which corresponds to symmetrical COO^- stretching modes, confirms a calcium oxalate monohydrate (COM) morphology for all the analyzed crystals [27-29]. This observation demonstrates a different chemical process currently occurring than the one presented in our earlier work, where a natural herbal infusion of *Larrea Tridentata* was used as the

inhibitor. While, previously, a structural modification of crystals from a COM for pure $CaC_2O_4{\cdot}(H_2O)_x$ to a dihydrate (COD) morphology for those grown with infusion was observed experimentally, no such morphological change is evident now. A closer inspection of these Raman spectra also reveals, for higher amounts of NDGA, decreases in the intensities of the bands around 500 and 600 cm^{-1}, which are associated with the wagging of CO_2 units, and of the peak at 1630 cm^{-1}, which corresponds to the symmetric COO^- stretching mode.

The Raman results in the frequency region of the most significant signature of COM structure, namely that of the peak doublet at 1465 and 1492 cm^{-1}, is presented in Fig. 4a. Despite the absence of a direct Raman detection of NDGA, these spectra demonstrate that some morphological changes still happen with increasing concentration of the inhibitor. There is a visible decrease in the intensity of the second peak at 1492 cm^{-1}, which corresponds to vibrational modes of twisted non-planar oxalate units [28], and it is marked with a solid arrow. Thus, with NDGA addition, such non-planar oxalate units are fewer in the new crystal configuration, resulting in this peak intensity decrease.

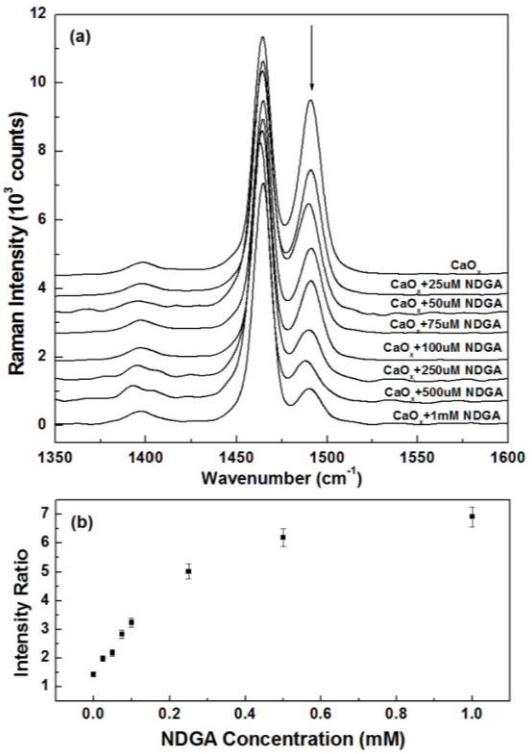

Figure 4. (a) Raman spectra in the frequency range of 1350 – 1600 cm^{-1} for crystals grown without, and with 25μM, 50μM, 75μM, 100μM, 250μM, 500μM, and 1mM NDGA inhibitor, as labeled. **(b)** Intensity ratio of 1465 and 1492 cm^{-1} peaks as a function of the added NDGA concentration.

While the effect is quite subtle at lower NDGA concentrations, the near disappearance of this feature is observed for the 1mM NDGA concentration. To better evaluate the influence of inhibitor addition in distorting the COM structure of the crystals, we present in Fig. 4b the intensity ratio of the 1465/1492 cm^{-1} peaks as a function of NDGA concentration. A nonlinear increase of this value from 1.4 for standard $CaC_2O_4{\cdot}(H_2O)_x$ crystals, to 3.2 for crystals grown with the addition of a 100μM concentration of NDGA, to a final value of about 7.0 for the addition of a 1mM NDGA concentration is revealed in Fig. 4b. Furthermore, it seems that a "saturation" limit of this ratio occurs for an NGDA concentration of 1mM, suggesting that using higher concentrations of NDGA would not make additional contributions to crystal morphological changes; NDGA would probably just remain in excess, agglomerating separately or coating the crystals.

A direct confirmation that NDGA is the chemical extract from the *Larrea Tridentata* plant is obtained through comparison of their IR transmission spectra (i.e., the spectrum of NDGA and the spectrum of the *Larrea Tridentata* herbal infusion), which are presented in Fig. 5a. Obtaining comparable Raman data was not achievable due to the high fluorescence of different organic compounds in the *Larrea Tridentata* herbal infusion. An overall trend, with similar absorption bands similar in the two spectra, is seen in Fig. 5a, validating that, indeed, NDGA is the main ingredient of *Larrea Tridentata*. To look for non-overlapping features in the IR spectra of standard $CaC_2O_4{\cdot}(H_2O)_x$ crystals and NDGA, in order to distinguish between the two compounds, we also present these spectra in Fig. 5b. For consistency and easier comparison, the same frequency range of 400 cm^{-1} to 3800 cm^{-1}, as in Fig. 5a, was used. This latter assessment will allow us to target appropriate spectroscopic regions in further investigating the influence of NDGA on crystals grown with the addition of inhibitor. Stronger overlap of characteristic IR vibrations of these compounds is seen in Fig. 5b in lower (wavenumbers < 1000 cm^{-1}) and higher (between 3000 and 3500 cm^{-1}) frequency regions. Consequently, the spectral region of 1000 – 2400 cm^{-1} was selected for our further analysis, with the results presented in Fig. 6. Also, comparison of the $CaC_2O_4{\cdot}(H_2O)_x$ infrared spectrum presented in Fig. 5b with literature data reveals a monohydrate structure [28,32,38] for the pure crystals, in agreement with the above Raman results. Moreover, by choosing the 1000 – 2400 cm^{-1} spectral region, an easier link to the Raman findings in Fig. 4a could be established, for a complete, complementary vibrational examination.

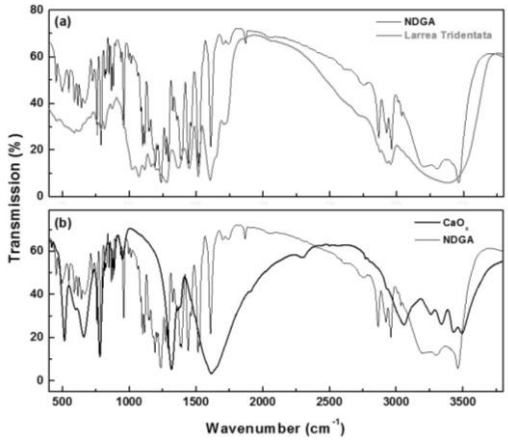

Figure 5. Infrared transmission spectra of: **(a)** NDGA and *Larrea Tridentata* and **(b)** standard calcium oxalate crystals and NDGA.

As can be observed in Fig. 6, there is no signature suggesting a structural change from monohydrate for crystals grown with inhibitor; all these IR spectra largely resemble that of pure $CaC_2O_4{\cdot}(H_2O)_x$ crystals shown in Fig. 5b. Thus, the IR data are in agreement with the Raman data of Fig. 4. In the context of a monohydrate structure of calcium oxalate, as previously mentioned, the most important vibrational signature in both spectroscopic techniques is a doublet peak, with active modes at

1465 and 1492 cm^{-1} in Raman and at 1316 and 1620 cm^{-1} in IR [27-29,36]. While NDGA has numerous absorption lines in this spectral region (see Fig. 5), in Fig. 6, only a single vibrational line at 1618 cm^{-1} exhibits increasing absorption intensity with increasing concentration of this compound. This observation, besides confirming the presence of NDGA, also clarifies a question that might arise in the assessment of morphological changes seen for crystals grown with this chemical extract, and that might result from IR and Raman data.

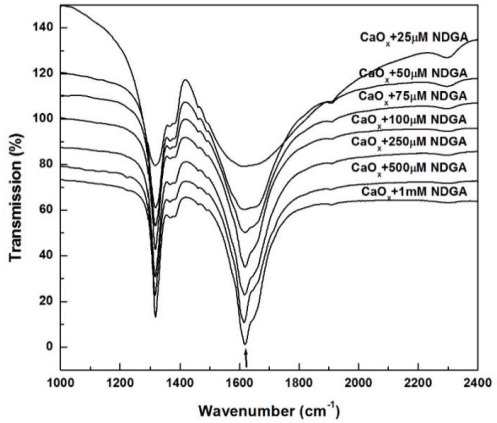

Figure 6. Infrared transmission spectra in the frequency range of 1000 – 2400 cm^{-1} of crystals grown with 25μM, 50μM, 75μM, 100μM, 250μM, 500μM, and 1mM NDGA inhibitor.

The two IR bands at 1316 and 1620 cm^{-1}, which are associated with symmetric and antisymmetric stretching modes of CO_2 units, respectively. While they have similar intensities in the IR spectrum of standard $CaC_2O_4{\cdot}(H_2O)_x$ crystals (see Fig. 5b), with the addition of more than 75μM NGDA, a slight increase is observed in the intensity of the 1620 cm^{-1} feature. However, not only is this band associated with an antisymmetric calcium oxalate IR mode, but also with the NDGA vibration at 1618 cm^{-1}; the latter definitely contributing to this feature's intensity increase. Also, because an IR absorption process is a one-photon direct process, and a Raman process is a two-photon scattering process involving electron-phonon interaction, the underlying principles contributing to the intensities of the expected symmetric and antisymmetric vibrational lines are quite different in these two techniques. Usually, in IR absorption measurements, antisymmetric vibrational modes are expected to dominate, with the symmetric modes more likely to be stronger in Raman measurements. Therefore, for crystals grown with NDGA, the observed intensity decrease of the symmetric stretching vibration at 1630 cm^{-1} previously seen in Raman results, and the intensity increase of the antisymmetric IR band at 1620 cm^{-1}, both demonstrate slight morphological changes in the structure of these crystals. In Raman results the vibrations associated with symmetric modes are going to be more affected, whereas those corresponding to antisymmetric vibrations will be more affected in the IR. Furthermore, since IR absorption is usually more sensitive in detecting low concentrations of analytes than is the Raman technique, the former is more likely to detect such a subtle NDGA presence.

Comparison with our previous results when the natural infusion from the plant was used and a change to a COD structure of $CaC_2O_4{\cdot}(H_2O)_x$ was observed, which is not the case with the current results, suggests that a key element is magnesium, which is known to be a constituent of the plant in general, and of chlorophyll in particular. Moreover, magnesium is considered to be the fourth most common element in the human body and the second most abundant intracellular cation [37]. Consequently, magnesium is essential in hundreds of metabolic pathways, including nephrological ones, and it is therefore important to consider the interaction between magnesium and kidney stone formation [38,39]. Magnesium has been previously described as a calcium oxalate kidney stone inhibitor [39-41]. However, some clinical trials reported conflicting results in using magnesium for antilithiasis therapy, despite its functionality as an inhibitor [42-44]. Magnesium inhibits calcium oxalate stone formation by competitively binding to oxalate, which prevents further calcium binding from taking place [39,40,45]. Magnesium oxalate formation thus occurs as a result. Due to magnesium oxalate's solubility in water, which is stronger than that of calcium oxalate (0.07g/100mL for magnesium oxalate versus 0.0007g/100mL for calcium oxalate), magnesium oxalate does not cause stone formation under physiological conditions [45]. Therefore, magnesium contributes to destabilizing calcium oxalate formation and also works synergistically with citrate in kidney stone inhibition [39,41,45].

4. CONCLUSIONS

The incidence rate and the recurrence rate of urolithiasis are still increasing worldwide. In the consideration of this, the present study consists of a comparative spectroscopic analysis of synthetically grown calcium oxalate calculi without and with addition of NDGA, which is a chemical extract of the *Larrea Tridentata* plant and is traditionally employed in the El Paso region as a natural treatment for kidney stones and bladder diseases. The research presented here is also a logical continuation of our previous efforts, where, by using traditional medicine (i.e., a natural infusion from *Larrea Tridentata* as a potential inhibitor), decreases in the average size of such crystals and changes in their structure from a monohydrate for pure crystals to a dihydrate for crystals grown with different amounts of inhibitor, were observed [25]. This research is a proactive analysis for trying to understand the difference between using a natural approach and using a chemical process for the calculi inhibition. The current study not only shows, through an infrared absorption investigation, that NDGA is, indeed, the main chemical extract from *Larrea Tridentata*, but also that a different inhibitory process is occurring when this chemical compound is used. The results obtained from both Raman and infrared absorption spectroscopic techniques reveal that NDGA is not responsible for the previously observed change in the structure of calcium oxalate crystals. The presence of NDGA slightly affects their morphology, which still resembles that of the monohydrate structure of standard $CaC_2O_4{\cdot}(H_2O)_x$ crystals. While a direct detection of NDGA in the crystallized calculi is not possible through Raman measurements due to the sensitivity limits of the technique, the presence of this compound is observed in the infrared absorption data, contributing to an increase in intensity of the antisymmetric IR band at 1620 cm^{-1}.

The decrease in the intensity of the Raman peak at 1492 cm^{-1} with increasing NDGA concentration suggests modification in the strength and length of the out-of-plane bonds of the twisted oxalate units of the COM morphology. Since this decrease exhibits a "saturation" limit at a 1mM concentration of NDGA, a higher NDGA concentration is unlikely to induce other important morphological changes; NDGA will just remain in excess and coat the surface of the crystals. Also, other Raman vibrations associated with symmetric modes, such as those around 500, 600, and 1630 cm^{-1}, again show decreases in their intensities.

In conclusion, while the main cause of inhibition using the natural infusion of *Larrea Tridentata* may well be the bonding of Mg^{2+} from the plant with oxalate ions from the crystal surface, the use of the NDGA chemical extract, which does not contain magnesium, demonstrates a different inhibitory process. If magnesium is liable for the previously seen structural change from COM to COD for crystals grown with natural extract addition, NDGA inhibitory effects only involve a distortion of the COM morphology. Keeping in mind that traditional herbal medicine is more affordable for prevention purposes, together with the fact that a larger amount of plant material is necessary in order to have a toxicological effect equivalent to that of a smaller amount of the chemical extract, this study confirms the value of the former approach. On the other hand, a deep understanding based on scientific knowledge is also of importance if we are seeking better clarification of the complicated mechanisms of the physiochemical processes that inhibit the formation of kidney stones

5. REFERENCES

1. Romero, V.; Akpinar, H.; Assimos, D.G. Kidney Stones: A Global Picture of Prevalence, Incidence, and Associated Risk Factors Kidney Stones: A Global Perspective. *Rev. Urol.* **2010**, *12*, 86–96.
2. Morgan, M.S.C.; Pearle, M.S. Medical management of renal stones. *BMJ* **2016**, *352*, 52, https://doi.org/10.1136/bmj.i52.
3. Luigia, M.; Summ, V. A Review of Pathological Biomineral Analysis Techniques and Classification Schemes. In *An Introduction to the Study of Mineralogy*; InTech, 2012, https://doi.org/10.5772/34861.
4. Saigal, C.S.; Joyce, G.; Timilsina, A.R. The Urologic Diseases in America Project "Direct and indirect costs of nephrolithiasis in an employed population: Opportunity for disease management?" *Kidney Int.* **2005**, *68*, 1808–1814, https://doi.org/10.1111/j.1523-1755.2005.00599.x.
5. Gottlieb, M.; Long, B.; Koyfman, A. The evaluation and management of urolithiasis in the ED: A review of the literature. *Am. J. Emerg. Med.* **2018**, *36*, 699–706, https://doi.org/10.1016/j.ajem.2018.01.003.
6. Sigurjonsdottir, V.K.; Runolfsdottir, H.L.; Indridason, O.S.; Palsson, R.; Edvardsson, V.O. Impact of nephrolithiasis on kidney function. *BMC Nephrol.* **2015**, *16*, https://doi.org/10.1186/s12882-015-0126-1.
7. Assimos, D. Kidney stones associate with increased risk for myocardial infarction. *J. Urol.* **2011**, *21*, 1641–1644.
8. Clayman, R.V. Obesity, Weight Gain, and the Risk of Kidney Stones. *J. Urol.* **2005**, *293*, 455–462.
9. Scales, C.D.; Smith, A.C.; Hanley, J.M.; Saigal, C.S. Prevalence of kidney stones in the United States. *Eur. Urol.* **2012**, *62*, 160–165, https://doi.org/10.1016/j.eururo.2012.03.052.
10. Taylor, E.N.; Stampfer, M.J.; Curhan, G.C. Diabetes mellitus and the risk of nephrolithiasis. *Kidney Int.* **2005**, *68*, 1230–1235, https://doi.org/10.1111/j.1523-1755.2005.00516.x.
11. Mikawlrawng, K.; Kumar, S. Current scenario of urolithiasis and the use of medicinal plants as antiurolithiatic agents in Manipur (North East India): A Review. *Int. J. Herb. Med. IJHM* **2014**, *2*, 1–12.
12. El-Zoghby, Z.M.; Lieske, J.C.; Foley, R.N.; Bergstralh, E.J.; Li, X.; Joseph Melton, L.; Krambeck, A.E.; Rule, A.D. Urolithiasis and the risk of ESRD. *Clin. J. Am. Soc. Nephrol.* **2012**, *7*, 1409–1415, https://doi.org/10.2215/CJN.03210312.
13. Rule, A.D.; Bergstralh, E.J.; Melton, L.J.; Li, X.; Weaver, A.L.; Lieske, J.C. Kidney stones and the risk for chronic kidney disease. *Clin. J. Am. Soc. Nephrol.* **2009**, *4*, 804–811, https://doi.org/10.2215/CJN.05811108.
14. Madore, F.; Stampfer, M.J.; Rimm, E.B.; Curhan, G.C. Nephrolithiasis and risk of hypertension. *Am. J. Hypertens.* **1998**, *11*, 46–53, https://doi.org/10.1016/s0895-7061(97)00371-3.
15. Coe, F.L.; Favus, M.J.; Aspin, J.R. Brenner and Rector's The Kidney. *Diabet. Nephropathy, 7th, BM Brenner. WB Saunders, Boston USA* **2004**, 1819–1866.
16. Pearle, M.S.; Calhoun, E.A.; Curhan, G.C. Urologic diseases in America project: urolithiasis. *J. Urol.* **2005**, *173*, 848–857, https://doi.org/10.1097/01.ju.0000152082.14384.d7.
17. Prasad, K.V.S.R.G.; Dodoala, S.; Koganti, B. Herbal drugs in urolithiasis-A review. *Pharmacogn. Rev* **2007**, *1*, 175–179.
18. Leusmann, D.B. A classification of urinary calculi with respect to their composition and micromorphology. *Scand. J. Urol. Nephrol.* **1991**, *25*, 141–150, http://dx.doi.org/10.3109/00365599109024549.
19. Rieu, P. Lithiases d'infection. *Ann. Urol. (Paris)* **2005**, *39*, 16–29.
20. Spencer, J.; Jacobs, J. Essential issues in complementary/alternative medicine. An Evidence-based Approach. *Complement. Altern. Med.* **1999**, *3*, 33–36, http://dx.doi.org/10.1054/ctim.2000.0360.
21. Newall, C.A.; Anderson, L.A.; Phillipson, J.D. Others Herbal medicines. A guide for health-care professionals. *J. Nat. Prod.* **1996**, *65*, 1964–1964.
22. Arteaga, S.; Andrade-Cetto, A.; Cárdenas, R. Larrea tridentata (Creosote bush), an abundant plant of Mexican and US-American deserts and its metabolite nordihydroguaiaretic acid. *J. Ethnopharmacol.* **2005**, *98*, 231–239, https://doi.org/10.1016/j.jep.2005.02.002.
23. Kasote, D.M.; Jagtap, S.D.; Thapa, D.; Khyade, M.S.; Russell, W.R. Herbal remedies for urinary stones used in India and China: A review. *J. Ethnopharmacol.* **2017**, *203*, 55–68, https://doi.org/10.1016/j.jep.2017.03.038.
24. Pinales, L.A.; Chianelli, R.R.; Durrer, W.G.; Pal, R.;

Narayan, M.; Manciu, F.S. Spectroscopic study of inhibition of calcium oxalate calculi growth by Larrea tridentata. *J. Raman Spectrosc.* **2011**, *42*, 259–264, https://doi.org/10.1002/jrs.2742.

25. Ghale-Salimi, M.Y.; Eidi, M.; Ghaemi, N.; Khavari-Nejad, R.A. Inhibitory effects of taraxasterol and aqueous extract of taraxacum officinale on calcium oxalate crystallization: In vitro study. *Ren. Fail.* **2018**, *54*, 252–257, https://doi.org/10.1080/0886022X.2018.1455595.

26. Manciu, F.S.; Govani, J.R.; Durrer, W.G.; Reza, L.; Pinales, L.A. Inhibition of urinary calculi - A spectroscopic study. *J. Raman Spectrosc.* **2009**, *40*, 861–865, https://doi.org/10.1002/jrs.2183.

27. Guerra-López, J.R.; Güida, J.A.; Della Védova, C.O. Infrared and Raman studies on renal stones: the use of second derivative infrared spectra. *Urol. Res.* **2010**, *38*, 383–390, https://doi.org/10.1007/s00240-010-0305-2.

28. Carmona, P.; Bellanato, J.; Escolar, E. Infrared and Raman spectroscopy of urinary calculi: A review. *Biospectroscopy* **1997**, *3*, 331–346, https://doi.org/10.1002/(SICI)1520-6343(1997)3:5<331::AID-BSPY2>3.0.CO;2-5.

29. Daudon, M.; Protat, M.F.; Reveillaud, R.J.; Jaeschke Boyer, H. Infrared spectrometry and Raman microprobe in the analysis of urinary calculi. *Kidney Int.* **1983**, *23*, 842–850, https://doi.org/10.1038/ki.1983.104.

30. Daudon, M.; Bader, C.; Jungers, P. Urinary calculi: review of classification methods and correlations with etiology. *Scanning Microsc.* **1993**, *7*, 1081–1104.

31. Grases, F.; Costa-Bauzá, A.; Ramis, M.; Montesinos, V.; Conte, A. Simple classification of renal calculi closely related to their micromorphology and etiology. *Clin. Chim. Acta* **2002**, *322*, 29–36, http://dx.doi.org/10.1016/S0009-8981(02)00063-3.

32. Tszzorl, V.; Dotvtbnecgbrrt, C. The crystal structures of whewellite and weddellite: re-examination and comparison. *Am. Mineral.* **1980**, *65*, 327–334.

33. Abou-Gazar, H.; Bedir, E.; Takamatsu, S.; Ferreira, D.; Khan, I.A. Antioxidant lignans from Larrea tridentata. *Phytochemistry* **2004**, *65*, 2499–2505, https://doi.org/10.1016/j.phytochem.2004.07.009.

34. Konno, C.; Lu, Z.-Z.; Xue, H.-Z.; Erdelmeier, C.A.J.; Meksuriyen, D.; Che, C.-T.; Cordell, G.A.; Soejarto, D.D.; Waller, D.P.; Fong, H.H.S. Furanoid Lignans from Larrea tridentata. *J. Nat. Prod.* **1990**, *53*, 396–406, http://dx.doi.org/10.1021/np50068a019.

35. Page, J.O. Determination of Nordihydroguaiaretic Acid in Creosote Bush. *Anal. Chem.* **1955**, *27*, 1266–1268.

36. Petrov, I.; Šoptrajanov, B. Infrared spectrum of whewellite. *Spectrochim. Acta Part A Mol. Spectrosc.* **1975**, *31*, 309–316, http://dx.doi.org/10.1016/0584-8539(75)80025-0.

37. Maguire, M.E.; Cowan, J.A. Magnesium chemistry and biochemistry. *BioMetals* **2002**, *15*, 203–210, https://doi.org/10.1023/A:1016058229972.

38. Cowan, J.A. Structural and catalytic chemistry of magnesium-dependent enzymes. *BioMetals* **2002**, *15*, 225–235, https://doi.org/10.1023/A:1016022730880.

39. Tavasoli, S.; Taheri, M.; Taheri, F.; Basiri, A.; Bagheri Amiri, F. Evaluating the associations between urinary excretion of magnesium and that of other components in calcium stone-forming patients. *Int. Urol. Nephrol.* **2019**, *51*, 279–284, https://doi.org/10.1007/s11255-018-2036-1.

40. Riley, J.M.; Kim, H.; Averch, T.D.; Kim, H.J. Effect of Magnesium on Calcium and Oxalate Ion Binding. *J. Endourol.* **2013**, *27*, 1487–1492, https://doi.org/10.1089/end.2013.0173.

41. Grases, F.; Rodriguez, A.; Costa-Bauza, A. Efficacy of Mixtures of Magnesium, Citrate and Phytate as Calcium Oxalate Crystallization Inhibitors in Urine. *J. Urol.* **2015**, *194*, 812–819, https://doi.org/10.1016/j.juro.2015.03.099.

42. Guerra, A.; Meschi, T.; Allegri, F.; Prati, B.; Nouvenne, A.; Fiaccadori, E.; Borghi, L. Concentrated urine and diluted urine: The effects of citrate and magnesium on the crystallization of calcium oxalate induced in vitro by an oxalate load. *Urol. Res.* **2006**, *34*, 359–364, https://doi.org/10.1007/s00240-006-0067-z

43. Kato, Y.; Yamaguchi, S.; Yachiku, S.; Nakazono, S.; Hori, J.I.; Wada, N.; Hou, K. Changes in urinary parameters after oral administration of potassium-sodium citrate and magnesium oxide to prevent urolithiasis. *Urology* **2004**, *63*, 7–11, http://dx.doi.org/10.1016/j.urology.2003.09.057.

44. Jaipakdee, S.; Prasongwatana, V.; Premgamone, A.; Reungjui, S.; Tosukhowong, P.; Tungsanga, K.; Suwantrai, S.; Noppawinyoowong, C.; Maskasame, S.; Sriboonlue, P. The effects of potassium and magnesium supplementations on urinary risk factors of renal stone patients. *J. Med. Assoc. Thail.* **2004**, *87*, 255–263.

45. Massey, L. Magnesium therapy for nephrolithiasis. *Magnes. Res.* **2005**, *18*, 123–126.

6. ACKNOWLEDGEMENTS

This work was supported by the NIH U01 NS090455 award, the NIH NIMHHD 2G12MD007592 award, The Grainger Foundation, and by a research agreement between the University of Texas at El Paso and the Mayo Clinic.